Published in final edited form as:
Plant Biotechnol J. 2014 October ; 12(8): 1098–1107. doi:10.1111/pbi.12217.

Structural and functional characterization of an anti-West Nile virus monoclonal antibody and its single-chain variant produced in glycoengineered plants

Huafang Lai[1,†], **Junyun He**[1,†], **Jonathan Hurtado**[1,2], **Jake Stahnke**[1,2], **Anja Fuchs**[3,&], **Erin Mehlhop**[5,$], **Sergey Gorlatov**[7], **Andreas Loos**[6], **Michael S. Diamond**[3,4,5], and **Qiang Chen**[1,2,*]

[1]The Biodesign Institute, Arizona State University, Tempe, AZ 85287

[2]School of Life Sciences, Arizona State University, Tempe, AZ 85287

[3]Department of Medicine, Washington University School of Medicine, St. Louis. MO 63110

[4]Department of Molecular Microbiology, Washington University School of Medicine, St. Louis. MO 63110

[5]Department of Pathology & Immunology, Washington University School of Medicine, St. Louis. MO 63110

[6]Department of Applied Genetics and Cell Biology, University of Natural Resources and Applied Life Sciences, Vienna, Austria

[7]MacroGenics, Inc, Rockville, MD 20850

Abstract

Previously, our group engineered a plant-derived monoclonal antibody (MAb pE16) that efficiently treated West Nile virus (WNV) infection in mice. In this study, we developed a pE16 variant consisting of a single-chain variable fragment (scFv) fused to the heavy chain constant domains (C_H) of human IgG (pE16scFv-C_H). pE16 and pE16scFv-C_H were expressed and assembled efficiently in *Nicotiana benthamiana* ΔXF plants, a glycosylation mutant lacking plant specific N-glycan residues. Glycan analysis revealed that ΔXF plant-derived pE16scFv-C_H (ΔXFpE16scFv-C_H) and pE16 (ΔXFpE16) both displayed a mammalian glycosylation profile. ΔXFpE16 and ΔXFpE16scFv-C_H demonstrated equivalent antigen binding affinity and kinetics, and slightly enhanced neutralization of WNV *in vitro* compared to the parent mammalian cell-produced E16 (mE16). A single dose of ΔXFpE16 or ΔXFpE16scFv-C_H protected mice against WNV-induced mortality even 4 days after infection at equivalent rates as mE16. This study provides a detailed tandem comparison of the expression, structure and function of a therapeutic MAb and its single-chain variant produced in glycoengineered plants. Moreover, it demonstrates the development of anti-WNV MAb therapeutic variants that are equivalent in efficacy to pE16, simpler to produce, and likely safer to use as therapeutics due to their mammalian N-

[*]Corresponding author: Qiang Chen, Ph.D., The Biodesign Institute, Arizona State University, 1001 S. McAllister Avenue, Tempe, Arizona 85287, USA T: (480) 239-7802, F: (480) 727-7615, qiang.chen.4@asu.edu.
[†]HL and JH contributed equally to this work.
[$]Current address: Department of Immunology, University of Washington, 750 Republican Street, Seattle WA 98109-8059
[&]Current address: Department of Pathology & Immunology, Washington University School of Medicine, St. Louis. MO 63110

glycosylation. This platform may lead to a more robust and cost effective production of antibody-based therapeutics against WNV infection and other infectious, inflammatory, or neoplastic diseases.

Keywords

Single-chain antibody; scFv-C_H; scFv-Fc; bifunctional MAb; C1q; Glycosylation; Glyco-engineering; Glycoengineered plants; Plant-made pharmaceuticals; Plant-made biologics; therapeutics; West Nile virus

Introduction

Although monoclonal antibodies (MAbs) produced in mammalian cell culture systems have achieved remarkable clinical success, their cost -intensive manufacturing has limited the availability, utility, and impact of these drugs. Plant-based expression systems offer opportunities to overcome these challenges due to their ability to produce recombinant proteins rapidly and at low cost (Chen, 2008; Chen, 2011). Production of functionally active MAbs requires a eukaryotic host cell as they require correct folding, assembly of two heavy chains (HC) and two light chains (LC), and complex posttranslational modifications including N-linked glycosylation. Plants have been shown to be an efficient system for expressing MAbs and their derivatives, such as IgG, IgA, diabodies, and recombinant immune complex (De Muynck et al., 2010; Phoolcharoen et al., 2011). However, the differences in N-linked glycosylation between MAbs produced in wild-type (WT) plants and mammalian cells has limited the use of plant-derived MAbs as human therapies, because non-native glycoforms could alter efficacy or result in plant-glycan specific immune responses that accelerate protein clearance or cause potential adverse effects through immune complex formation. To overcome this challenge, glycosylation pathways in several protein production-host plants including *Nicotiana benthamiana* have been glycoengineered to produce mammalian-type N-linked glycans by genetically suppressing or eliminating enzymes for the biosynthesis of plant-specific glycans and by introducing glycoenzymes from mammalian cells (Castilho and Steinkellner, 2012; Loos and Steinkellner, 2012). For example, a *N. benthamiana* plant line (ΔXF) was generated by RNA interference (RNAi) technology to silence expression of the endogenous β1,2-xylosyltransferase and a1,3-fucosyltransferase genes (Strasser et al., 2008). *N*-glycan analysis showed that ΔXF line-produced endogenous glycoproteins exhibited a profile of complex-type *N*-glycans with markedly reduced levels of a1,3-fucose and virtually no plant-specific xylose on endogenous proteins (Strasser et al., 2008). Moreover, MAbs produced in this plant line have a homogenous mammalian N-glycoform with terminal N-acetylglucosamine (Gn) residues (i.e. GnGn structures), lacking unwanted β1,2-xylose and core a1,3-fucose residues (Strasser et al., 2008).

West Nile virus (WNV) is a positive-stranded, enveloped RNA virus that infects the central nervous system (CNS) of human and animals. Once a disease that was restricted to Old World countries, it has spread across the United States (US), Canada, the Caribbean region and Latin America with more frequent and severe outbreaks of neuroinvasive disease in

recent years (Petersen et al., 2013). Currently, no vaccine or therapeutic agent has been approved for human use. The lack of treatment for the global WNV epidemic calls for the development of effective and low-cost antiviral therapeutics. We previously reported a plant-derived, humanized murine MAb (pE16) with post-exposure therapeutic activity against WNV (Lai et al., 2010; Lai et al., 2012). We demonstrated that pE16 protected mice from WNV infection and mortality equivalently compared to mammalian cell-produced E16 (mE16) in both pre- and post-exposure treatment models (Lai et al., 2010). While successful, pE16 was produced in wild-type (WT) *N. benthamiana* plants, and this, potentially had the undesirable effects of plant-specific N-glycans as human therapy. In addition, two sets of deconstructed viral vectors based on *Tobacco mosaic virus* (TMV) and *Potato virus X* (PVX) were used to drive the expression of HC and LC, respectively (Giritch et al., 2006). This required the co-infiltration of 5 *Agrobacterium* strains and a careful control of the ratio of TMV/PVX modules for the optimal expression and assembly of pE16. This complicates the operational process, raises the production cost, and increases regulatory compliance burden in establishing and validating multiple *Agrobacterium* banks. From a manufacturing and safety perspective, it would be desirable to produce pE16 with mammalian N-glycoforms, and to develop pE16 variants, such as a single-chain variable fragment (scFv) of pE16 fused to the HC constant domain (C_H) of human IgG (pE16scFv-C_H), that only require one expression vector while retaining therapeutic potency.

Here, we expressed pE16 and pE16scFv-C_H in the glycoengineered *N. benthamiana* plant line ΔXF that modifies proteins with a mammalian-type N-glycan (GnGn). We demonstrated that ΔXF plants expressed and assembled pE16 and pE16scFv-C_H efficiently. Glycan analysis confirmed that ΔXF plant-derived pE16 (ΔXFpE16) and pE16scFv-C_H (ΔXFpE16scFv-CH) carried mammalian-type N-linked glycans. ΔXFpE16 and ΔXFpE16scFv-C_H exhibited enhanced neutralization against WNV infection and showed equivalent protection as the parent mE16 against a lethal WNV challenge in a mouse model even 4 days after infection. Furthermore, the ΔXFpE16scFv-CH variant expressed and protected equivalently as ΔXFpE16, and eliminated the challenge of balancing the ratio of TMV/PVX modules for optimal expression and assembly of HC and LC. Overall, this study provides a detailed analysis of the expression, structure and function of a therapeutic MAb and its single-chain variant produced in a glycoengineered plants. Moreover, it demonstrates anti-WNV MAb therapeutic variants generated in glycoengineered plants are equivalent in efficacy to the parent pE16, but are more cost effective to produce, and likely safer to use as therapy in humans because of their mammalian N-linked glycosylation.

Results

Expression and assembly of pE16 and pE16scFv-C_H in ΔXF *N. benthamiana*

We initially demonstrated that pE16 and pE16scFv-C_H could be expressed and assembled equivalently in ΔXF *N. benthamiana* as in WT plants. ΔXF is a *N. benthamiana* RNAi based glycosylation mutant that lacks plant specific xylose and core fucose residues, thus synthesizing mainly GnGn structures (Strasser et al., 2008). *Agrobacterium tumefaciens* strains containing the pE16 (Lai et al., 2010) or pE16scFv-C_H construct (He et al., 2014) were co-delivered into ΔXF *N. benthamiana* leaves along with the promoter module and an

integrase construct through agroinfiltration (Chen et al., 2013; Leuzinger et al., 2013). Expression of ΔXFpE16 and ΔXFpE16scFv-C_H was monitored by Western blotting under reducing or non-reducing conditions. Both ΔXpE16 and ΔXpE16scFv-C_H were expressed in leaves of ΔXF *N. benthamiana* with the expected molecular weight (Fig 1A, **Lanes 2- 3**), and assembled into the expected heterotetramer (ΔXFpE16) or dimer (ΔXFpE16scFv-C_H) (Fig 1B, **Lanes 2–3).** Maximum expression of ΔXFpE16 and ΔXFpE16scFv-CH was reached 7–8 days post infiltration (dpi), with an average accumulation of 0.74 and 0.77 mg/g leaf fresh weight (LFW), respectively (Fig 2). These levels are similar to those obtained in WT *N. benthamiana* plants reported previously (He et al., 2014; Lai et al., 2010). We also extracted ΔXFpE16 and ΔXFpE16scFv-C_H from leaves with a scalable purification process that was previously developed for pE16 produced in WT plants (WTpE16) (Lai et al., 2010). Both ΔXFpE16 and ΔXFpE16scFv-C_H were extracted efficiently from plant tissue and enriched to >90% purity by a combination of ammonium sulfate precipitation and protein A chromatography steps (Fig 1C, **Lanes 2 and 3**). Purified ΔXFpE16 and ΔXFpE16scFv-C_H were used for further functional characterization.

ΔXFpE16 and ΔXFpE16scFv-C_H exhibited mammalian N-linked glycosylation patterns

A typical feature of human IgG1-type antibodies is a conserved N-glycosylation site at asparagine 297 (Asn_{297}) in the C_H2 domain; the presence of N-linked glycosylation at this site affects stability and effector functions (Houde et al., 2010). Since both ΔXFpE16 and ΔXFpE16scFv-C_H encode this N-linked glycosylation site, we examined their glycosylation status by liquid-chromatography-electrospray ionization-mass spectrometry (LC-ESI-MS). ΔXFpE16 exhibited the expected mammalian-type complex N-glycan GnGn with a high degree (~ 95%) of uniformity (Fig 3A). GnGn structures also were the major glycoform of ΔXFpE16scFv-C_H (Fig 3B). However, substantial amounts of endoplasmic reticulum (ER) typical oligomannosidic structures, predominantly Man8 and Man9, were present (Fig 3B). Notably, no plant-specific glycan residues (i.e. β1,2-xylose and core a1,3-fucose) were detected in either ΔXF-expressed antibody. Homogeneous mammalian-type glycosylation and the lack of plant-specific glycans should eliminate the risk of their immunogenicity in humans and enhance their safety profile as therapeutic MAbs. mE16 displayed core a1,6 fucosylated structures with and without terminal galactose (Fig 3C).

Antigen binding and neutralization activity of ΔXFpE16 and ΔXFpE16scFv-C_H

Antigen binding kinetics and affinity of ΔXFpE16 and ΔXFpE16scFv-C_H were investigated by several assays. Binding to WNV envelope (E) protein was first determined by ELISA with purified WNV E protein coated in the solid phase on microtiter plates (Lai et al., 2010). ΔXFpE16 and ΔXFpE16scFv-C_H showed specific binding to WNV E compared to the reference mE16 MAb (Fig 4). Antigen binding of ΔXFpE16 and ΔXFpE16scFv-C_H was investigated more quantitatively using surface plasmon resonance (SPR) with purified domain III of the WNV E protein (DIII) immobilized on a BIAcore chip (Lai et al., 2010). As shown in Fig 5, ΔXFpE16 and ΔXFpE16scFv-C_H had very similar binding affinities and kinetics to monovalent DIII of WNV E compared to mE16 (K_D of 18.6 to 25 nM). These results confirm that pE16 and pE16scFv-C_H with mammalian N-linked glycoforms have equivalent antigen binding activity as mE16.

The neutralization potential of ΔXFpE16 and ΔXFpE16scFv-C_H was evaluated by a quantitative neutralization assay that measures MAb inhibition of infection with WNV reporter virus particles (RVPs) (Lai et al., 2010; Pierson et al., 2006). ΔXFpE16 was slightly more potent in neutralizing WNV infection than mE16 and WTpE16 (Fig 6, Table 1). ΔXFpE16scFv-C_H neutralized WNV infection equivalently compared to mE16 (Fig 6B, Table 1). To investigate if the complement component C1q augmented the neutralizing activity of ΔXFpE16 and ΔXFpE16scFv-C_H, purified C1q was included during the virus-MAb incubation stage (Fig 6, Table 1). In the presence of C1q, the neutralization curves of mE16 and ΔXFpE16scFv-C_H (Fig 6B and C) but not WTpE16 or ΔXFpE16 (Fig 6A and D) shifted to the left, suggesting modestly or significantly greater WNV neutralization potency of ΔXFpE16scFv-C_H and mE16 in the presence of C1q, respectively. The difference in C1q augmentation between these E16 variants likely reflects the variation in their N-linked glycosylation status, which impacts their ability to interact with C1q (Lai et al., 2010; Mehlhop et al., 2009). Overall, ΔXFpE16 and ΔXFpE16scFv-C_H retained potent neutralizing activity against infectious WNV.

ΔXFpE16 and ΔXFpE16scFv-C_H have prophylactic and therapeutic potential against lethal WNV infection

Five week-old wild type C57BL/6 mice ($n > 10$, per group) were used in prophylaxis studies to evaluate the concentrations of ΔXFpE16, ΔXFpE16scFv-C_H, and mE16 that prevent WNV infection. The New York 2000 strain of WNV (10^2 PFU) was inoculated in mice subcutaneously, which has been shown previously to cause an 80 to 90% mortality rate in this model (Engle and Diamond, 2003). On the same day of infection, increasing amounts (1 to 1000 ng) of ΔXFpE16, ΔXFpE16scFv-C_H or 100 ng of mE16 were administered as a single dose. Notably, 70 to 100% of mice were protected from lethal infection when 100 ng of ΔXFpE16 or ΔXFpE16scFv-C_H was administered ($P < 0.01$), whereas the same dose of mE16 protected 80% of mice (Fig 7A). Thus, there was no statistically significant difference in protection between ΔXFpE16, ΔXFpE16scFv-C_H and mE16 at this dose ($P > 0.7$). Mortality also was reduced by a single injection of as low as 10 ng of ΔXFpE16 or ΔXFpE16scFv-C_H (Fig 7A). The survival rate for 100 ng of ΔXFpE16 appeared to be higher than that of 1 μg treatment in these experiments. However, the difference between the two dosages is not statistically significant ($P > 0.3$).

Post-exposure therapeutic treatments were performed by passively administering a single dose of ΔXFpE16, ΔXFpE16scFv-C_H or mE16 4 days after subcutaneous inoculation of 102 PFU of WNV. This time point was chosen because prior studies have shown that WNV has spread to the brain in these mice by day 4 after infection (Oliphant et al., 2005). Since our previous data showed that 50 μg - 500 μg WTpE16 was protective in the mouse model (He et al., 2014; Lai et al., 2010), the same dosage range was used for ΔXFpE16 and ΔXFpE16scFv-C_H. For example, 85% of mice were protected from lethal infection when a single dose of 500 μg of ΔXFpE16scFv-C_H was given 4 days after WNV inoculation, similar to the protection observed with the same dose of mE16 (80%) (Fig 7B, $P > 0.7$). A single dose of 50 μg of ΔXFpE16 at day 4 also protected equivalently compared to mE16 (80%) (Fig 7B, $P > 0.8$). ΔXFpE16scFv-C_H also protected mice similarly as mE16 at this lower dosage (data not shown). Overall, ΔXFpE16 and ΔXFpE16scFv-C_H, which were

produced in plants and displayed mammalian N-linked glycans, had equivalent prophylactic and therapeutic efficacy in mice compared to the original mE16.

Discussion

Plants offer an alternative production system to overcome the high-cost and low-capacity challenges of the current mammalian cell culture-based manufacturing systems for MAbs (Chen, 2008; Chen, 2011; De Muynck et al., 2010). The recent development of transient expression systems based on deconstructed viral vectors has further increased the speed and yield of MAb production and positioned plant-based systems as a leading contender for MAb manufacturing (Chen et al., 2011; Giritch et al., 2006; Huang et al., 2009; Lico et al., 2008). For example, high levels of MAbs (0.5 – 1mg/g LFW) can be produced in *N. benthamiana* and lettuce plants within 10 days of vector infiltration by using the MagnICON and geminiviral vectors (He et al., 2012; He et al., 2014; Huang et al., 2010; Lai et al., 2010; Lai et al., 2012; Phoolcharoen et al., 2011; Zeitlin et al., 2011). While lower manufacturing cost has been widely assumed for plant-based production platforms due to the lack of need for capital investments to build sophisticated cell culture facilities and expensive culture media for biomass generation, accurate documentation on the actual cost of producing plant-made biologics (PMBs) in industry scales was scarce in scientific literature. However, a very recent study on two plant-made enzymes that represent PMBs of diverse applications provided the urgently needed technoeconomic evaluations of the current PMB platform and offered solid support for the cost-saving benefit of PMBs (Tuse et al., 2014). For example, using reported data and SuperPro Designer® modeling software, it was calculated that the unit production costs for the plant-made human butyrylcholinesterase (BuChE) for use as a medical countermeasure was approximately $234 or $474 per dose, respectively depending on if Facility Dependent Costs are included in the estimation (Tuse et al., 2014). This is in stark contrast to the ~$10,000/dose production cost reported for BuChE in the current manufacturing system (Tuse et al., 2014). Similarly, the study demonstrated that production of cellulase in plants for ethanol production may result in a >30% reduction in unit production costs and an 85% reduction in the required capital investment compared with the current fungal-based system (Tuse et al., 2014). Since *Agrobacterium* is a Gram-negative bacterium, it is crucial to monitor and remove endotoxins that may be introduced into the feed stream by *Agrobacterium* during agroinfiltration. As reported previously (He et al., 2014; Lai et al., 2010; Lai et al., 2012), our purification scheme can effectively remove endotoxins from the MAb proteins to levels that were below specifications by the United States Food and Drug Administration (FDA) for injectable MAb pharmaceuticals (data not shown).

We previously demonstrated the efficacy of a plant-derived MAb pE16 as a post-exposure therapeutic against WNV (Lai et al., 2010; Lai et al., 2012). Since pE16 was produced in WT *N. benthamiana* plants, WTpE16 consequentially carried plant-typical N-glycans, which differ from mammalian-type N-glycans by the presence of β1,2-xylose and core a1,3-fucose and the lack of terminal β1,4-galactose and sialic acid residues (Bosch et al., 2013; Gomord et al., 2010). These differences may alter MAb efficacy as N-linked glycosylation of the Fc region modulates the binding and activation of C1q and Fc-γ receptors (FcγRs) (Houde et al., 2010). The difference in N-linked glycosylation also raises concerns for the

immunogenicity of WT plant-derived MAb therapeutics, as they might induce plant-glycan specific immune responses that reduce therapeutic efficacy by accelerating MAb clearance from plasma or worse, cause adverse effects through immune complex formation. To overcome these issues, we expressed pE16 and its single chain variant E16scFv-C_H in the glycoengineered *N. benthamiana* plant line ΔXF that decorates glycoproteins with the mammalian-type complex *N*-glycan GnGn (Strasser et al., 2008). Our results demonstrated that ΔXFpE16 and ΔXFpE16scFv-C_H were expressed and assembled as efficiently as WTpE16 with similar kinetics and yield. Importantly, glycan analysis indicated that ΔXF plant-derived pE16 molecules displayed mammalian forms of N-linked glycans. ΔXFpE16 had no detectable plant-specific N-glycans and 95% of ΔXFpE16 had the predicted mammalian glycoform GnGn. This high glycan homogeneity contrasts to that of human embryonic kidney 293 (HEK-293) cell-produced mE16 (Lai et al., 2010), as mE16 had a mixture of several glycoforms. This result is consistent with previous reports showing that MAbs produced in glycoengineered *N. benthamiana* plants had mammalian-type N-linked glycoforms and superior glycan homogeneity compared to their mammalian cell-produced counterparts (Zeitlin et al., 2011). The lack of terminal sialic acids in the N-glycans of mE16 (Fig 3C) further illustrated that protein N-glycosylation in mammalian cells could be affected by culture conditions and may have significant batch-to-batch variation. The high degree of glycan homogeneity of plant-produced MAbs may translate into better activity *in vitro* and *in vivo* depending on particular functional mechanisms. Glycan uniformity also provides the opportunity to study the impact of specific carbohydrate constituents on MAb function and correspondingly to select glycoforms with enhanced efficacy, stability, or safety. Moreover, the ability to produce consistently glycosylated MAbs for therapeutic applications is highly significant from both a quality and regulatory perspective.

ΔXFpE16scFv-C_H also exhibited mammalian glycoforms and had no detectable plant-specific glycans. However, in addition to 40% of GnGn, 52% were of oligomannosidic structures (Man8 and Man9-types) that are shared by plant and mammalian glycoproteins. This incomplete glycan processing indicates aberrant localization in ER or ER-derived vesicles for this population of ΔXFpE16scFv-C_H, even though this molecule was targeted for secretion and not tagged with an ER-retention signal, such as KDEL. This result was not unexpected, as it was previously observed that a secretion-targeted scFv-C_H exhibited predominantly ER-type oligomannosidic N-linked glycans when produced in WT plants (He et al., 2014). A similar observation of oligomannosidic glycoforms and aberrant subcellular deposition also was reported for Arabidopsis (*Arabidopsis thaliana*) seed-derived scFv-Fcs (Loos et al., 2011). Previous studies suggested that the altered glycosylation and localization of scFv variants were due at least partially to the lack of the LC constant region (C_L) in these constructs, as co-expression of LC and the paring of C_L and C_H1 reduced the percentage of oligomannosidic glycans in scFv-C_H (Feige et al., 2009; He et al., 2014). However, the impact of structural variations in the IgG backbone on N-linked glycosylation may involve additional factors and warrants further investigation. Overall, the mammalian N-linked glycoforms of ΔXFpE16 and ΔXFpE16scFv-C_H eliminate their risk of immunogenicity and other undesirable effects associated with plant-specific glycans, and facilitate their application as human therapeutics against WNV.

To our knowledge, this study provides the first tandem comparison of the expression, structure and function of a therapeutic monoclonal antibody and its single-chain variant produced in plants. ΔXFpE16 and ΔXFpE16scFv-C_H had a similar expression pattern and yield, and antigen-binding activity comparable to mE16. ΔXFpE16 was at least equivalent if not slightly more potent than mE16 in neutralizing WNV in the absence of C1q (EC_{5O}: 3.7 ng/ml vs. 9.2 ng/ml), whereas ΔXFpE16scFv-C_H neutralized WNV infection equivalently compared to mE16. The enhanced neutralizing activity of ΔXFpE16 may be attributed to its high glycan homogeneity or the difference in N-linked glycan structures between ΔXFpE16, ΔXFpE16scFv-C_H, and mE16. Previously, two anti-HIV MAbs with a highly homogeneous β1,4-galactosylated (AA) N-glycan profile were observed to have improved virus neutralization activity (Strasser et al., 2009). Studies have shown that the complement component C1q enhances the neutralizing potency of mE16 (Mehlhop et al., 2009). However, C1q did not augment the neutralizing potency of WTpE16 or ΔXFpE16. We previously showed that WTpE16 carried plant-specific β1,2-xylose and core a1,3-fucose residues on its complex N-linked glycans which conferred lower binding to C1q and consequently impaired the augmenting effect of C1q (He et al., 2014; Lai et al., 2010). We speculate that the impairment of C1q augmentation in ΔXFpE16 also may be due to its particular N-linked glycosylation pattern. For ΔXFpE16scFv-C_H, C1q did lower its EC_{50} by ~ 2-fold. This suggests that the population of ΔXFpE16scFv-C_H that displayed oligomannosidic N-glycans might be responsible for the partial preservation of C1q augmentation. If true, oligomannosidic glycoforms of pE16 with improved neutralization potency can be produced readily in plants by tagging the HC C-terminus with the ER-retention signal KDEL. In spite of their difference in neutralization potency, ΔXFpE16 and ΔXFpE16scFv-C_H showed virtually equivalent and potent protection relative to the parent mE16 against a lethal WNV infection in a mouse model. It is possible that the lack of C1q augmentation for ΔXFpE16 *in vivo* was compensated by its slightly greater neutralizing activity in the absence of C1q. Overall, these results demonstrated the potency of ΔXFpE16 and ΔXFpE16scFv-C_H in protecting mice against a lethal WNV challenge even 4 days after infection when WNV has already disseminated into the brain.

The equivalent therapeutic potency *in vivo* also suggests that ΔXFpE16scFv-C_H may be a desirable alternative to pE16 as a therapeutic agent. ΔXFpE16scFv-C_H combines the advantages of both scFvs and full MAb molecules. The presence of C_H in the fusion molecule preserves the bivalency, pharmacokinetics and effector functions of a complete MAb. Its smaller size, however, may offer superior tissue penetration, a feature that is useful for reaching our long-term goal of increasing the efficacy of pE16 by enhancing its penetration across the blood-brain barrier (BBB). The smaller size of ΔXFpE16scFv-C_H and the demonstration of its therapeutic potency suggest that it may be possible to develop IgG-like bifunctional MAbs that assemble from two scFvs with distinct binding specificities. For example, one of the two scFvs could bind to a specific receptor (e.g., insulin receptor (Boado et al., 2007)) on the BBB to facilitate transport into the brain, and the other scFv would retain its binding and neutralization against WNV in the brain. Such pE16 bifunctional MAbs are currently in development and might prolong the window of efficacy.

From a manufacturing perspective, the production of ΔXFpE16scFv-C_H is simpler and could be more cost-effective than pE16. Expression of pE16 requires two set of deconstructed viral vectors to promote expression of HC and LC, respectively (Lai et al., 2010). In turn, it requires the engineering of two molecular constructs (HC and LC), the establishment and validation of 5 *Agrobacterium* banks, and the coinfiltration of 5 *Agrobacterium* strains into plant leaves. It also demands careful control of the *Agrobacterium* ratio of HC/LC modules for optimal expression and assembly of pE16. These requirements complicate the manufacturing process, may raise the production cost, and increase regulatory compliance burdens. While major production cost of biologics are associated with downstream processing, upstream processes including the establishment, characterization and validation of master *Agrobacterium* banks especially under current Good Manufacture Practices (cGMP) regulations can also incur substantial cost for their production. For example, one typical mammalian cell bank for MAb costs approximately $ 350,000 – 500,000 to establish (Rasmussen et al., 2012). The manufacturing cost for establishing a cGMP master *Agrobacterium* bank is assumed to be less expensive than that of mammalian cells due to the reduced cost in fermenter and culture media; however, it still incurs the equivalent labor and regulatory compliance costs in charactering and validating the identity, stability and functionality of the bank. Since the production of ΔXFpE16scFv-C_H only requires one expression vector, accordingly, it would simplify the operational process, help to reduce the overall cost of goods, and provide a more robust platform for large-scale manufacturing of anti-WNV or other MAb-based therapeutics in plants.

Experimental Procedures

Expression of pE16 MAb and pE16scFv-C_H in ΔXF *N. benthamiana* leaves

The construction of pE16 HC and pE16 LC in pICH11599 and pICH21595 and the construction of pE16scFv-C_H in pICH11599 have been described previously (He et al., 2014; Lai et al., 2010). Plant expression vectors were individually transformed into *A. tumefaciens* GV3101 by electroporation as previously described (Santi et al., 2008). ΔXF *N. benthamiana* plants were grown and agroinfiltrated or co-agroinfiltrated with GV3101 strains containing the pE16scFv-C_H or pE16 HC/pE16 LC 3′ modules along with their respective 5′ modules and an integrase construct as described previously to express pE16 variants (Chen, 2013; Chen et al., 2013; Lai and Chen, 2012; Lai et al., 2010; Leuzinger et al., 2013).

Extraction and purification of pE16 variants from ΔXF *N. benthamiana* leaves

To evaluate the temporal pattern of ΔXFpE16 and ΔXFpE16scFv-C_H expression, agroinfiltrated ΔXF *N. benthamiana* leaves were harvested 4–12 dpi. Leaves were harvested 7 dpi (ΔXFpE16) or 8 dpi (ΔXFpE16scFv-C_H) for ΔXFpE16 and ΔXFpE16scFv-C_H purification and other analysis. Extraction and purification of ΔXFpE16 and ΔXFpE16scFv-C_H from plant leaves were performed using a method previously reported for WTpE16 MAb (Lai et al., 2010). Briefly, leaves were homogenized in extraction buffer (PBS, 1mM EDTA, 10 mg/ml sodium ascorbate, 10 μg/ml leupeptin, and 0.3 mg/ml PMSF). The extract was clarified by centrifugation at 17,700 × *g* for 30 min at 4°C and purified by a two-step

purification process comprised of ammonium sulfate precipitation and protein A affinity chromatography.

SDS-PAGE, Western blot, and ELISA

Samples containing ΔXFpE16 and ΔXFpE16scFv-C_H were subjected to 10% SDS-PAGE under reducing (5% v/v β-mercaptoethanol) or to 4–20% gradient SDS-PAGE under non-reducing conditions. Gels were either stained with Coomassie blue or used to transfer proteins onto PVDF membranes. A polyclonal antibody conjugated with horseradish peroxidase (HRP) against human-gamma HC (Southern Biotech) was used for western blot analysis as previously described (Lai et al., 2010). The expression and antigen binding of ΔXFpE16 and ΔXFpE16scFv-C_H were examined by ELISA as described previously (Lai et al., 2010). Briefly, E ectodomain (amino acids 1 to 415) or DIII (amino acids 296–415) of the New York 1999 strain of WNV was purified from *E. coli* (Oliphant et al., 2007) and immobilized on microtiter plates. After incubation with plant protein extract or purified ΔXFpE16 or ΔXFpE16scFv-C_H, an HRP-conjugated anti-human-gamma HC antibody (Southern Biotech) was used to detect bound antibodies. The plates were then developed with TMB substrate (KPL Inc). mE16 (Oliphant et al., 2005) was used as a reference standard.

N-linked glycan analysis

N-linked glycosylation analysis was carried out by LC-ESI-MS as described previously (Stadlmann et al., 2008). Briefly, MAb variants were purified and separated by reducing SDS-PAGE. Gels were stained with Coomassie, the HC containing bands were excised from the gel, subjected to S-alkylation and tryptic or tryptic/GluC digestion. MAb fragments were eluted from the gel with 50% acetonitrile and separated on a Reversed Phase Column (150 × 0.32 mm BioBasic-18, Thermo Scientific) with a gradient of 1%–80% acetonitrile. Glycopeptides were analyzed with a quadruple time-of-flight (Q-TOF) Ultima Global mass spectrometer (Waters, Milford, MA, USA). Summed and deconvoluted spectra were used for glycoform identification. Glycans were annotated according to the ProGlycAn nomenclature (www.proglycan.com).

Surface plasmon resonance

Affinity measurement of E16 MAb or its variant for DIII of WNV was performed by SPR (BIAcore 3000 biosensor, GE, Healthcare). WNV DIII was immobilized on the CM-5 sensor chip (150 RU) by an amine coupling kit as recommended by the manufacturer. Subsequently, purified ΔXFpE16, ΔXFpE16scFv-CH or mE16 was injected at concentrations of 6.25, 12.5, 25, 50 and 100 nM, a flow rate of 30 μl/minute for 120 sec, and then allowed to dissociate over 120 sec. Regeneration of naked antigen surfaces was performed by pulse injection of 10 mM glycine pH 1.5. All binding experiments were performed in 10 mM HEPES, pH 7.4, 150 mM NaCl, 3 mM EDTA, and 0.005% P20 surfactant. Binding responses were analyzed using the BIA evaluation 4.1 software. Kinetic constants, $k_{(a)}$ and $k_{(d)}$, were estimated by global fitting analysis of the association/dissociation curves to the Bivalent analyte interaction model. The equilibrium dissociation constant (KD) was calculated as $KD=k_{(d)}/k_{(a)}$.

Neutralization assay

WNV reporter virus particles (RVP) were produced in HEK293T cells (Pierson et al., 2006; Pierson et al., 2007). WNV RVPs were mixed with varying concentrations (0.24 – 16,000 ng/ml) of WTpE16, ΔXFpE16, ΔXFpE16scFv-C_H or mE16 in the presence of medium or 50 μg/ml purified human C1q protein (Complement Technologies) and then incubated with permissive Raji-DC-SIGN-R cells. Forty hours later, cells were fixed and analyzed by flow cytometry for GFP expression (Pierson et al., 2006; Pierson et al., 2007). Neutralization was monitored as a function of GFP fluorescence.

Efficacy of MAbs in mice

C57BL/6 mice were housed in a pathogen-free mouse facility. Studies were performed with approval from the Washington University School of Medicine Animal Safety Committee. Mice received a single dose of purified ΔXFpE16, ΔXFpE16scFv-C_H or mE16 by intraperitoneal injection the same day or four days after footpad infection with 10^2 PFU of WNV strain 3000.0259. Kaplan-Meier analysis of survival data was performed using the log-rank test. Statistical significance was determined using a log-rank test.

Acknowledgments

We thank M. Engle and R. Sun for their assistance in mouse efficacy studies and in plant biomass generation, respectively. We also thank Drs. F. Altmann and H. Steinkellner of BOKU Vienna, Austria, for assisting in glycan analysis and data interpretation. The continuous support for undergraduate research by Dr. D. Green of Arizona State University is greatly appreciated. This work was supported by a NIAID grants number U01 AI075549 and R21 AI101329 to Q. Chen. H. Lai and J. He contributed equally to this publication.

References

Boado RJ, Zhang Y, Zhang Y, Pardridge WM. Humanization of anti-human insulin receptor antibody for drug targeting across the human blood-brain barrier. Biotechnol Bioeng. 2007; 96:381–391. [PubMed: 16937408]

Bosch D, Castilho A, Loos A, Schots A, Steinkellner H. N-Glycosylation of Plant-produced Recombinant Proteins. Current Pharmaceutical Design. 2013; 19:5503–5512. [PubMed: 23394562]

Castilho A, Steinkellner H. Glyco-engineering in plants to produce human-like N-glycan structures. Biotechnology Journal. 2012; 7:1088–1098. [PubMed: 22890723]

Chen Q. Expression and Purification of Pharmaceutical Proteins in Plants. Biological Engineering. 2008; 1:291–321.

Chen, Q. Expression and manufacture of pharmaceutical proteins in genetically engineered horticultural plants. In: Mou, B.; Scorza, R., editors. Transgenic Horticultural Crops: Challenges and Opportunities - Essays by Experts. Boca Raton: Taylor & Francis; 2011. p. 83-124.

Chen, Q. Virus-like Particle Vaccines for Norovirus Gastroenteritis. In: Giese, M., editor. Molecular Vaccines. Vienna: Springer; 2013. p. 153-181.

Chen Q, He J, Phoolcharoen W, Mason HS. Geminiviral vectors based on bean yellow dwarf virus for production of vaccine antigens and monoclonal antibodies in plants. Hum Vaccin. 2011; 7:331–338. [PubMed: 21358270]

Chen Q, Lai H, Hurtado J, Stahnke J, Leuzinger K, Dent M. Agroinfiltration as an Effective and Scalable Strategy of Gene Delivery for Production of Pharmaceutical Proteins. Advanced Technolgy in Biology and Medicine. 2013; 1:103–112.

De Muynck B, Navarre C, Boutry M. Production of antibodies in plants: status after twenty years. Plant Biotechnology Journal. 2010; 8:529–563. [PubMed: 20132515]

Engle M, Diamond MS. Antibody prophylaxis and therapy against West Nile Virus infection in wild type and immunodeficient mice. J Virol. 2003; 77:12941–12949. [PubMed: 14645550]

Feige MJ, Groscurth S, Marcinowski M, Shimizu Y, Kessler H, Hendershot LM, Buchner J. An unfolded CH1 domain controls the assembly and secretion of IgG antibodies. Mol Cell. 2009; 34:569–579. [PubMed: 19524537]

Giritch A, Marillonnet S, Engler C, van Eldik G, Botterman J, Klimyuk V, Gleba Y. Rapid high-yield expression of full-size IgG antibodies in plants coinfected with noncompeting viral vectors. Proc Natl Acad Sci U S A. 2006; 103:14701–14706. [PubMed: 16973752]

Gomord V, Fitchette AC, Menu-Bouaouiche L, Saint-Jore-Dupas C, Plasson C, Michaud D, Faye L. Plant-specific glycosylation patterns in the context of therapeutic protein production. Plant Biotechnology Journal. 2010; 8:564–587. [PubMed: 20233335]

He J, Lai H, Brock C, Chen Q. A Novel System for Rapid and Cost-Effective Production of Detection and Diagnostic Reagents of West Nile Virus in Plants. Journal of Biomedicine and Biotechnology. 2012; 2012:1–10. [PubMed: 21836813]

He J, Lai H, Engle M, Gorlatov S, Gruber C, Steinkellner H, Diamond MS, Chen Q. Generation and Analysis of Novel Plant-Derived Antibody-Based Therapeutic Molecules against West Nile Virus. PLoS ONE. 2014; 9:e93541. DOI:93510.91371/journal.pone.0093541. [PubMed: 24675995]

Houde D, Peng Y, Berkowitz SA, Engen JR. Post-translational modifications differentially affect IgG1 conformation and receptor binding. Mol Cell Proteomics. 2010; 9:1716–1728. [PubMed: 20103567]

Huang Z, Chen Q, Hjelm B, Arntzen C, Mason H. A DNA replicon system for rapid high-level production of virus-like particles in plants. Biotechnol Bioeng. 2009; 103:706–714. [PubMed: 19309755]

Huang Z, Phoolcharoen W, Lai H, Piensook K, Cardineau G, Zeitlin L, Whaley K, Arntzen CJ, Mason H, Chen Q. High-level rapid production of full-size monoclonal antibodies in plants by a single-vector DNA replicon system. Biotechnol Bioeng. 2010; 106:9–17. [PubMed: 20047189]

Lai H, Chen Q. Bioprocessing of plant-derived virus-like particles of Norwalk virus capsid protein under current Good Manufacture Practice regulations. Plant Cell Reports. 2012; 31:573–584. [PubMed: 22134876]

Lai H, Engle M, Fuchs A, Keller T, Johnson S, Gorlatov S, Diamond MS, Chen Q. Monoclonal antibody produced in plants efficiently treats West Nile virus infection in mice. Proc Natl Acad Sci U S A. 2010; 107:2419–2424. [PubMed: 20133644]

Lai H, He J, Engle M, Diamond MS, Chen Q. Robust production of virus-like particles and monoclonal antibodies with geminiviral replicon vectors in lettuce. Plant Biotechnology Journal. 2012; 10:95–104. [PubMed: 21883868]

Leuzinger K, Dent M, Hurtado J, Stahnke J, Lai H, Zhou X, Chen Q. Efficient Agroinfiltration of Plants for High-level Transient Expression of Recombinant Proteins. Journal of Visualized Experiments. 201310.3791/50521

Lico C, Chen Q, Santi L. Viral vectors for production of recombinant proteins in plants. J Cell Physiol. 2008; 216:366–377. [PubMed: 18330886]

Loos A, Steinkellner H. IgG-Fc glycoengineering in non-mammalian expression hosts. Arch Biochem Biophys. 2012; 526:167–173. [PubMed: 22634260]

Loos A, Van Droogenbroeck B, Hillmer S, Grass J, Pabst M, Castilho A, Kunert R, Liang M, Arcalis E, Robinson DG, Depicker A, Steinkellner H. Expression of antibody fragments with a controlled N-glycosylation pattern and induction of endoplasmic reticulum-derived vesicles in seeds of Arabidopsis. Plant physiology. 2011; 155:2036–2048. [PubMed: 21325568]

Mehlhop E, Nelson S, Jost CA, Gorlatov S, Johnson S, Fremont DH, Diamond MS, Pierson TC. Complement protein C1q reduces the stoichiometric threshold for antibody-mediated neutralization of West Nile virus. Cell host & microbe. 2009; 6:381–391. [PubMed: 19837377]

Oliphant T, Engle M, Nybakken G, Doane C, Johnson S, Huang L, Gorlatov S, Mehlhop E, Marri A, Chung KM, Ebel GD, Kramer LD, Fremont DH, Diamond MS. Development of a humanized monoclonal antibody with therapeutic potential against West Nile virus. Nature Medicine. 2005; 11:522–530.

Oliphant T, Nybakken GE, Austin SK, Xu Q, Bramson J, Loeb M, Throsby M, Fremont DH, Pierson TC, Diamond MS. Induction of epitope-specific neutralizing antibodies against West Nile virus. J Virol. 2007; 81:11828–11839. [PubMed: 17715236]

Petersen LR, Brault AC, Nasci RS. West Nile virus: review of the literature. Jama. 2013; 310:308–315. [PubMed: 23860989]

Phoolcharoen W, Bhoo SH, Lai H, Ma J, Arntzen CJ, Chen Q, Mason HS. Expression of an immunogenic Ebola immune complex in Nicotiana benthamiana. Plant Biotechnology Journal. 2011; 9:807–816. [PubMed: 21281425]

Pierson TC, Sanchez MD, Puffer BA, Ahmed AA, Geiss BJ, Valentine LE, Altamura LA, Diamond MS, Doms RW. A rapid and quantitative assay for measuring antibody-mediated neutralization of West Nile virus infection. Virology. 2006; 346:53–65. [PubMed: 16325883]

Pierson TC, Xu Q, Nelson S, Oliphant T, Nybakken GE, Fremont DH, Diamond MS. The stoichiometry of antibody-mediated neutralization and enhancement of West Nile virus infection. Cell host & microbe. 2007; 1:135–145. [PubMed: 18005691]

Rasmussen SK, Naested H, Muller C, Tolstrup AB, Frandsen TP. Recombinant antibody mixtures: production strategies and cost considerations. Arch Biochem Biophys. 2012; 526:139–145. [PubMed: 22820097]

Santi L, Batchelor L, Huang Z, Hjelm B, Kilbourne J, Arntzen CJ, Chen Q, Mason HS. An efficient plant viral expression system generating orally immunogenic Norwalk virus-like particles. Vaccine. 2008; 26:1846–1854. [PubMed: 18325641]

Stadlmann J, Pabst M, Kolarich D, Kunert R, Altmann F. Analysis of immunoglobulin glycosylation by LC-ESI-MS of glycopeptides and oligosaccharides. Proteomics. 2008; 8:2858–2871. [PubMed: 18655055]

Strasser R, Castilho A, Stadlmann J, Kunert R, Quendler H, Gattinger P, Jez J, Rademacher T, Altmann F, Mach L, Steinkellner H. Improved Virus Neutralization by Plant-produced Anti-HIV Antibodies with a Homogeneous b1,4-Galactosylated N-Glycan Profile. Journal of Biological Chemistry. 2009; 284:20479–20485. [PubMed: 19478090]

Strasser R, Stadlmann J, Schahs M, Stiegler G, Quendler H, Mach L, Glossl J, Weterings K, Pabst M, Steinkellner H. Generation of glyco-engineered Nicotiana benthamiana for the production of monoclonal antibodies with a homogeneous human-like N-glycan structure. Plant Biotechnology Journal. 2008; 6:392–402. [PubMed: 18346095]

Tuse D, Tu T, McDonald K. Manufacturing Economics of Plant-Made Biologics: Case Studies in Therapeutic and Industrial Enzymes. Biomed Res Int. 2014; 2014:10. (http://www.hindawi.com/journals/bmri/aip/256135/).

Zeitlin L, Pettitt J, Scully C, Bohorova N, Kim D, Pauly M, Hiatt A, Ngo L, Steinkellner H, Whaley KJ, Olinger GG. Enhanced potency of a fucose-free monoclonal antibody being developed as an Ebola virus immunoprotectant. Proc Natl Acad Sci U S A. 2011; 108:20690–20694. [PubMed: 22143789]

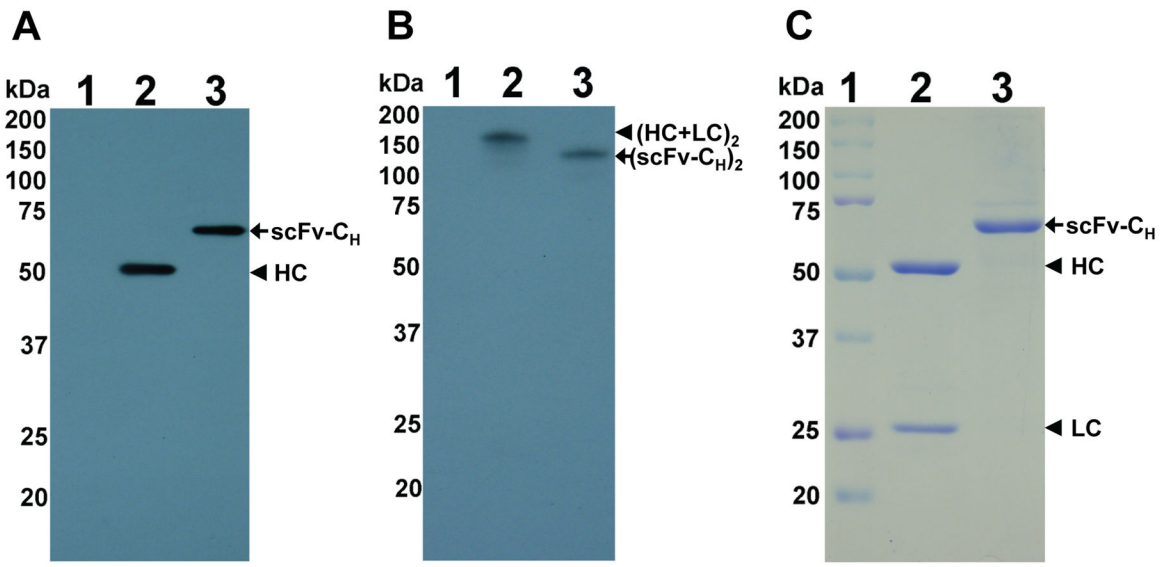

Figure 1. Expression and purification of ΔXFpE16 and ΔXFpE16scFv-C_H. A and B
Western blot analysis. ΔXFpE16 and ΔXFpE16scFv-C_H were extracted from ΔXF *N. benthamiana* leaves, separated on SDS-PAGE gels under reducing (**A**) or non-reducing (**B**) conditions, and blotted onto PVDF membranes. A goat anti-human gamma chain antibody was incubated with the membranes to detect ΔXFpE16 (**Lane 2**) or ΔXFpE16scFv-C_H (**Lane 3**). Protein sample extracted from ΔXF leaves infiltrated with buffer was used as negative control **(Lane 1). C.** Molecular weight standard (**Lane 1**), purified ΔXFpE16 (**Lane 2**) and ΔXFpE16scFv-C_H (**Lane 3**) were separated on a 4–20% gradient SDS-PAGE gel under reducing condition and visualized with Coomassie blue stain. HC: heavy chain, scFv: single-chain variable fragment; C_H: the constant region of HC; LC: light chain; (HC +LC)$_2$: fully assembled heterotetrameric form of IgG; (scFv-C_H)$_2$: dimer of scFv-C_H.

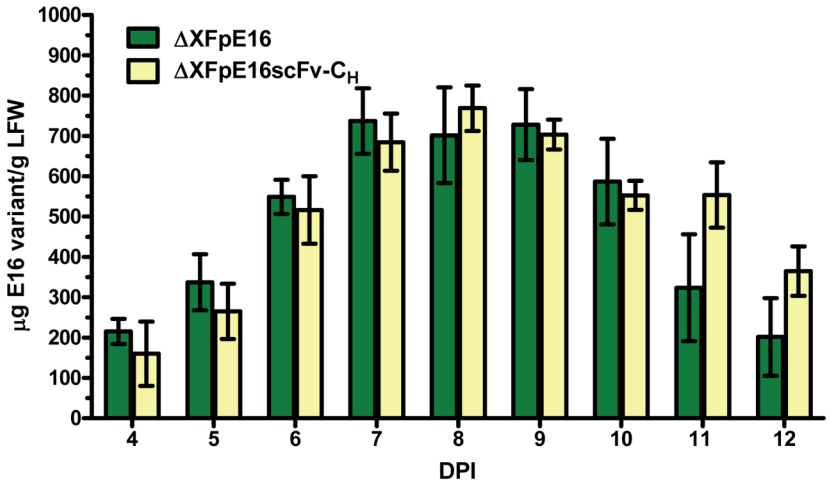

Figure 2. Temporal expression patterns of ΔXFpE16 and ΔXFpE16scFv-C_H

Total protein from ΔXF plant leaves co-infiltrated or infiltrated with pE16 HC and LC or pE16scFv-C_H construct was extracted on days 4–12 post infiltration and analyzed by ELISA that detects the assembled form of ΔXFpE16 and ΔXFpE16scFv-C_H. Mean ± SD of samples from three independent infiltrations are presented.

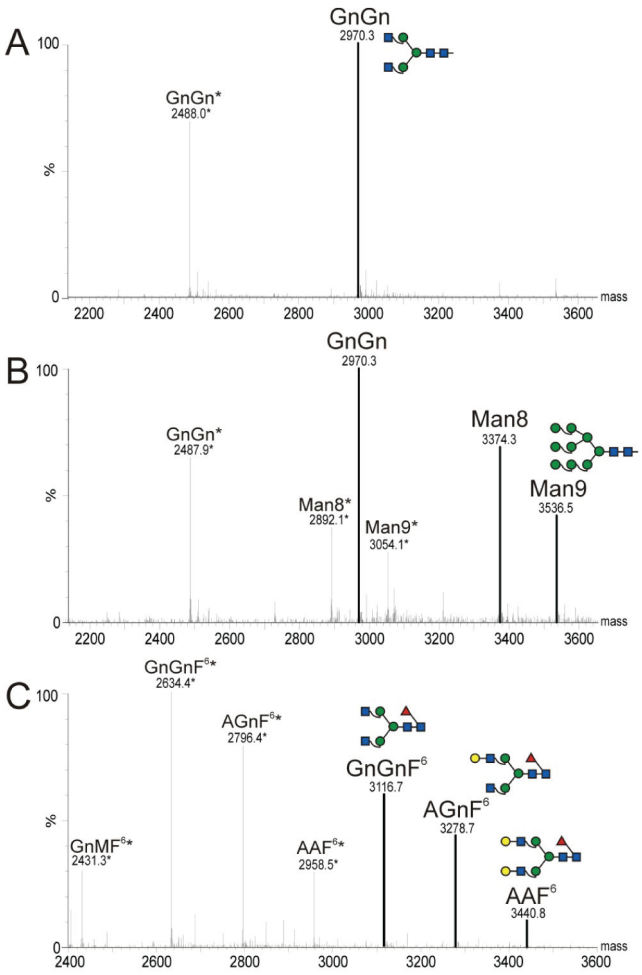

Figure 3. N-linked glycan analysis of E16 antibody variants

Glycosylated peptides containing the Asn_{297} residue of the C_H region were obtained from purified ΔXFpE16 (**A**), ΔXFpE16scFv-C_H (**B**), or mE16 (**C**) by tryptic digestion, and analyzed by LC-ESI-MS. Note, ΔXF is a *N. benthamiana* N-glycosylation mutant, that decorates proteins with mammalian type GnGn glycans. Glycans were annotated according to the ProGlycAn nomenclature (www.proglycan.com). Due to an incomplete tryptic digestion two glycopeptides were generated that differ by 482 Da (Loos and Steinkellner, 2012). Glycopeptide (GP) 1 is indicated with an asterisk, GP 2 is highlighted.

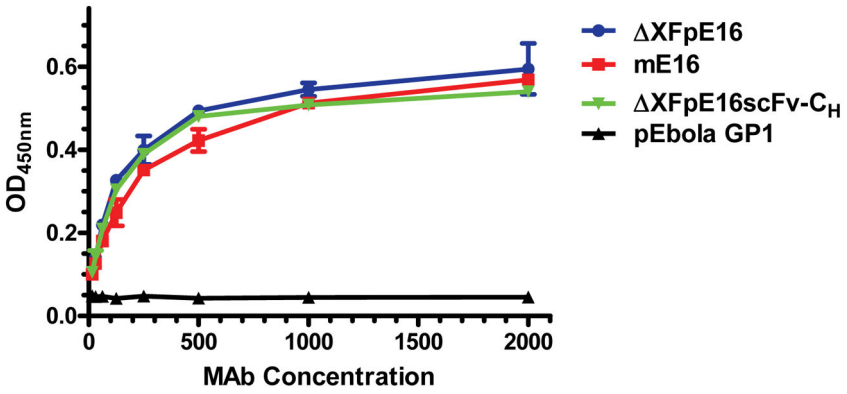

Figure 4. Antigen-binding ELISA of ΔXFpE16 and ΔXFpE16scFv-C_H to WNV E

Serial dilutions of ΔXFpE16 and ΔXFpE16scFv-C_H were incubated on plates coated with WNV E and detected with an HRP-conjugated anti-human gamma antibody. Dilutions of mE16 were used in parallel as reference standards. A plant-produced anti-Ebola glycoprotein (GP1) MAb (pEbola GP1) (Huang et al., 2010) was used as a negative control. Mean ± SD of samples from three independent experiments is presented. Error bars for ΔXFpE16scFv-CH (SD = 0.003 – 0.014) and pEbola GP1 (SD = 0.001 – 0.007) were too small to be visible.

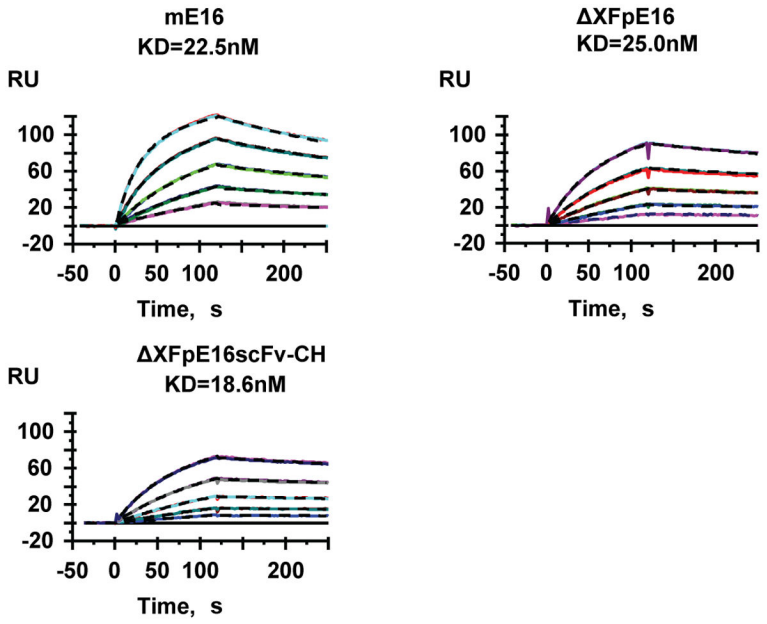

Figure 5. Surface plasmon resonance analysis of binding kinetics and affinity of ΔXFpE16 and ΔXFpE16scFv-C_H to WNV DIII

ΔXFpE16, ΔXFpE16scFv-C_H or mE16 was injected over WNV DIII fragment immobilized to the CM-5 biosensor chip. The black dashed lines represent the global fit to Bivalent analyte model of binding curves obtained at concentrations of 6.25, 12.5, 25, 50 or 100 nM. A representative set of SPR binding curves from several independent experiments is shown.

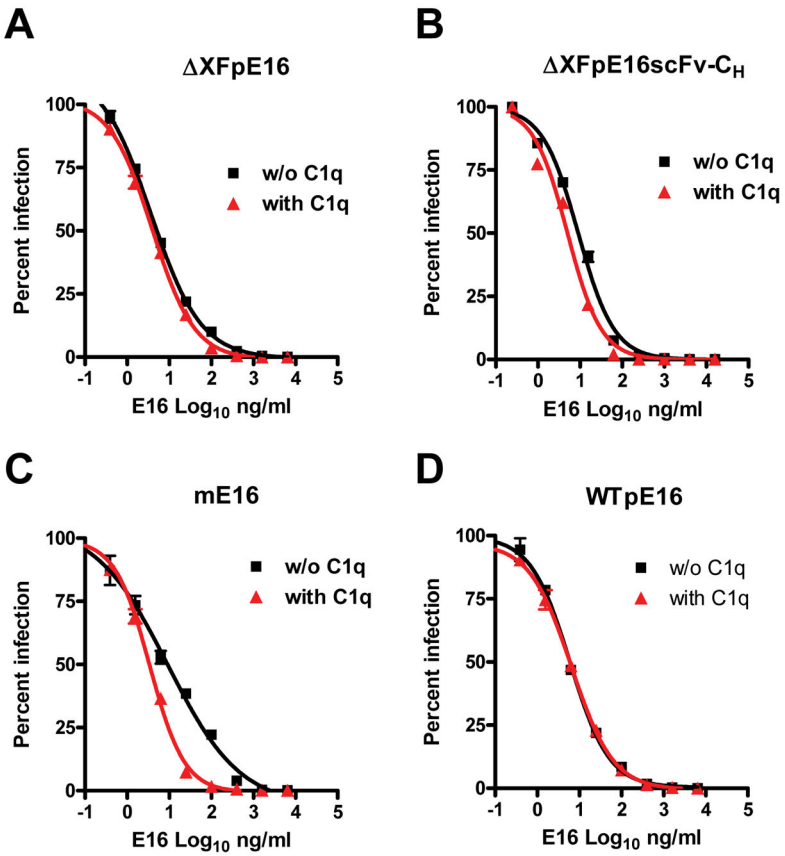

Figure 6. Neutralization of WNV by ΔXFpE16 and ΔXFpE16scFv-C_H

WNV RVPs were pre-incubated with serial dilutions of ΔXFpE16 (**A**),ΔXFpE16scFv-C_H (**B**), mE16 (**C**, control 1), or WTpE16 (**D**, control 2) in the presence of medium (w/o C1q, black line) or 50 μg/ml of human C1q (with C1q, red line), and used to infect permissive Raji-DC-SIGN-R cells. After 40 hours of incubation, cells were fixed and analyzed by flow cytometry for GFP expression. Data are representative of at least two independent experiments.

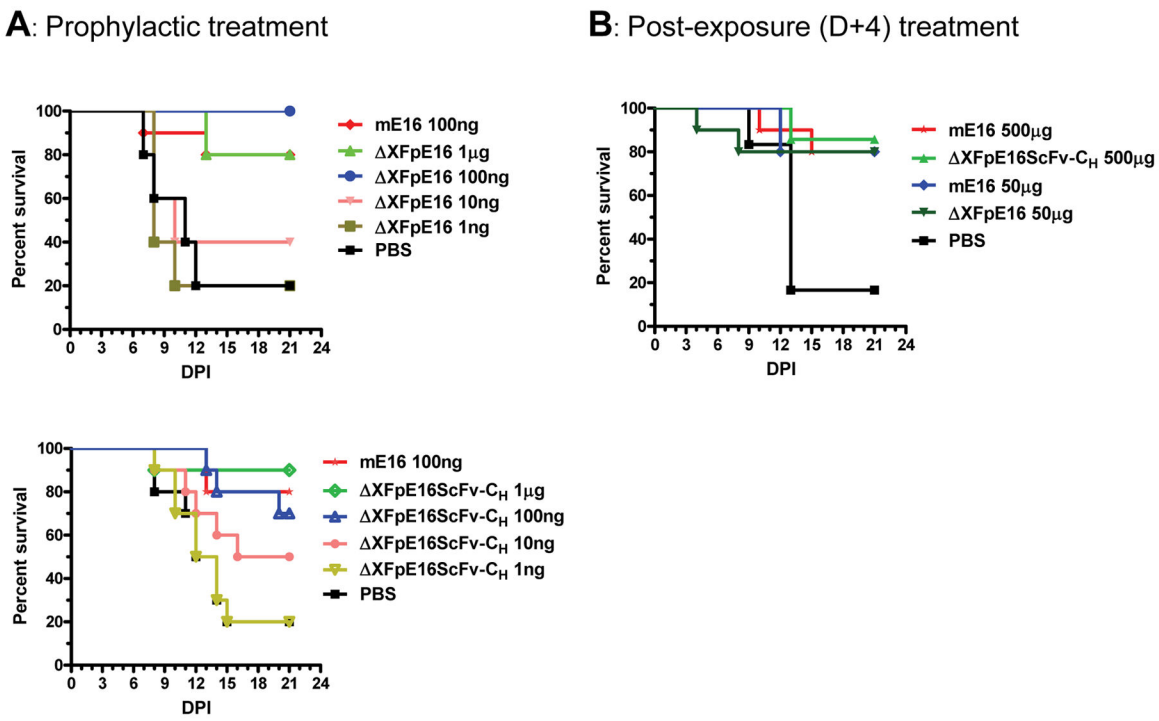

Figure 7. ΔXFpE16 and ΔXFpE16scFv-C_H mediated protection in mice

A. Five week-old C57BL/6 mice were passively transferred saline, or serial increases in dose (ranging from 1 to 1000 ng, *n*=10 mice per dose) of ΔXFpE16 or ΔXFpE16scFv-C_H via an intraperitoneal route on the same day as subcutaneous infection with 10^2 PFU of WNV. Survival data from at least two independent experiments were analyzed by log-rank test. mE16 (100 ng) was used in parallel as a positive control. **B**. Wild type C57BL/6 mice were infected with 10^2 PFU of WNV and then given a single dose of ΔXFpE16 (50 μg), ΔXFpE16scFv-C_H (500 μg) or mHu-E16 (50 μg or 500 μg) via an intraperitoneal route at day +4 after infection. Survival data from at least two independent experiments (*n* = 10 mice per dose) were analyzed by the log-rank test.

Table 1
Neutralization activity of E16 MAb variants

ΔXFpE16: E16 MAb produced in ΔXF *N. benthamiana* plants, ΔXFpE16scFv-CH: E16 MAb scFv-CH variant produced in ΔXF *N. benthamiana* plants, WTpE16: E16 MAb produced in wild-type *N. benthamiana* plants, mE16: E16 MAb produced in mammalian cells.

E 16 samples	ΔXFpE16	ΔXFpE16scFv-CH	WTpE16	mE16
EC50 (ng/ml) without C1q	3.7	9.1	6.0	9.2
EC50 (ng/ml) with C1q	3.9	5.0	6.5	3.4